

Novel Calibration Method for Switched Capacitor Arrays Enables Time Measurements with Sub-Picosecond Resolution

D. A. Stricker-Shaver, S. Ritt and B. J. Pichler

Abstract—Switched capacitor arrays ASICs are becoming more and more popular for the readout of detector signals, since the sampling frequency of typically several gigasamples per second allows excellent pile-up rejection and time measurements. They suffer however from the fact that their sampling bins are not equidistant in time, given by limitations of the chip process. In the past, this limited time measurements of optimal signals to about 5-25 ps in accuracy, depending on the specific chip, even after careful time calibrations. This paper introduces a novel time calibration, which allows pushing this limit below 1 ps, and also determines the true sampling speed. Various test measurements with different boards based on the DRS4 ASIC indicate that the new calibration is valid over a wide temperature range and stable over time.

Index Terms—Time Calibration, DRS4, Switched Capacitor Array, Analog memory

I. INTRODUCTION

SWITCHED CAPACITOR ARRAYS (SCA) are application specific integrated circuits (ASIC) which allow transient analog signal recording at high sampling speeds. They have been first used for particle detector readout back in the 1980's as shown by Kleinfelder [1]. The principle is to use an array of capacitors in sample-and-hold mode. A fast sequence of write pulses allows the recording of analog waveforms in these capacitors, which can later be read out and digitized at a much lower speed. While early chips used shift registers to generate the write pulses, it was soon realized that using inverter chains as delay lines boost the sampling speed into the gigasamples per second (GSPS) region as demonstrated in [2]. Following the advances in CMOS technology, SCAs have become faster over the years, and current chip versions from different groups allow sampling speeds in the range of 2-15 GSPS [3]-[6]. They have signal-to-noise ratios (SNR) of 10-13 bits equivalent and sampling depths of 256 to 64k cells. Paired with typical power consumptions of 10 mW per channel, these chips are excellent alternatives for commercial flash-ADCs. They all share however the disadvantage that the time required to read out the capacitor cells causes dead time. Depending on the number

of channels and cells to read out, this dead time is in the typical range of 10-100 micro seconds, which limits the application to cases where one can use a trigger to limit the number of events to typically 100-1000 events/s. The field of application for SCAs therefore lies in areas where one has a low trigger rate, but requires excellent time resolution and pile-up rejection. This includes for example particle physics at the intensity frontier [7], Cherenkov telescopes in gamma-ray astronomy [8], time-of-flight (TOF) applications [9] and neutrino physics [10]. Also, in medical imaging, specifically in positron emission tomography (PET), where TOF plays an important role [11], SCAs are a candidate for future applications. In [12] a coincident resolving time (CRT) of 100 ps (FWHM) was demonstrated for PET signals using LaBr₃ as a scintillator. This represents a single time resolution of ~30 ps (RMS) and requires precise electronics to measure this time.

Several TOF measurements have been made recently with various SCA chips. In the readout of micro channel plates, a single detector resolution of ~15 ps (RMS) has been achieved, which is comparable with the best commercial combination of constant-fraction-discriminators with time-to-amplitude converters, but at a much lower cost per channel [13]. The readout of straw tubes [14] via a time measurement gave good results, although the accuracy was limited by the imperfect time calibration (TC) method used for the SCA chip.

Over many years, the general opinion was that time measurements with SCA chips are limited to about 5-25 ps (RMS), caused by the time jitter inside the chips. The authors have found however that SCA chips can perform much better if the correct TC is applied. This allows pushing the achievable time resolution by about one order of magnitude to below one picosecond.

II. THEORY OF OPERATION

Most modern SCAs use a kind of inverter chain to generate the write pulses which open analog switches to sample the input signal. Fig. 1 shows a simplified schematics of the DRS4 chip, which is the fourth generation in a family of SCA developed at PSI [5]. The advantage of this technique is that a simple inverter chain used as a tapped delay line can run much faster than any shift register, easily reaching 10-20 GSPS with modern chip technologies. The disadvantage however is that the transition time of an inverter depends on parameters like temperature and supply voltage. To address this problem, most

This work was supported in part by the Deutsche Forschungsgemeinschaft (DFG) Grant Nr. PI771/3-1 and Swiss Werner Siemens Foundation.

D. A. Stricker-Shaver and B. J. Pichler are with Werner Siemens Imaging Center, University of Tübingen, Tübingen, Germany.

S. Ritt is with Paul Scherrer Institute (PSI), Villigen, Switzerland (e-mail: stefan.ritt@psi.ch).

SCAs use a delay-locked loop (DLL) or a phase locked loop (PLL) to stabilize the sampling frequency to an external constant reference clock.

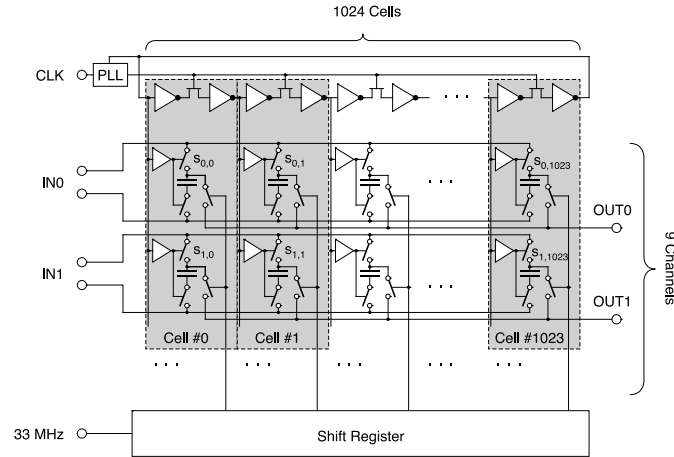


Fig. 1: Simplified schematics of the DRS4 chip.

Furthermore, mismatch between transistors in the CMOS process causes each inverter to have different but fixed transition times even if the other parameters are kept constant. Since this effect comes from the actual geometrical size of a transistor and its doping properties, it is stable over time and can be corrected for by measuring the transition time of each inverter and correcting for it. This measurement and its correction is the main topic of this paper and will be detailed in chapter IV.B.

III. LIMITATIONS OF TIME MEASUREMENTS

After a proper TC, the accuracy of a time measurement with a SCA chip is limited by the residual random jitter of the transition time of the inverter chain. Each inverter has a voltage threshold at the input. Crossing this threshold turns the inverter high or low. While this threshold is very stable, any noise on the input signal will cause a time jitter of the inverter. Careful chip design allows minimizing this noise, causing modern SCA chips to have typical inverter chain time jitters below 1 ps.

To measure the arrival time of a certain electrical pulse e.g. in particle physics, the pulse time is typically extracted from the rising respectively falling edge of the waveform. The simplest case is to use a single threshold discriminator. In the case of waveform digitizing, the equivalent can be achieved in the digital domain by comparing the digitized voltage of the sampling points with a fixed value. To achieve a time resolution exceeding the sampling interval, adjacent samples can be interpolated linearly or with cubic functions. In Fig. 2a an interpolated line from an ideal signal intersects a given threshold at time t_l depicted by an open square. Any voltage noise on the measured signal causes time jitter as shown in Fig. 2b. If some voltage noise “rises” the signal by an amount Δu , the linearly interpolated line intersects the same threshold at a time t_l' different from t_l , as depicted by the grey square. From Fig. 2b one can easily derive the formula for the time accuracy Δt as

$$\frac{\Delta u}{\Delta t} = \frac{U}{t_r}, \quad (1)$$

where U is the signal height, t_r the rise time and Δu the voltage noise as shown in Fig. 2.

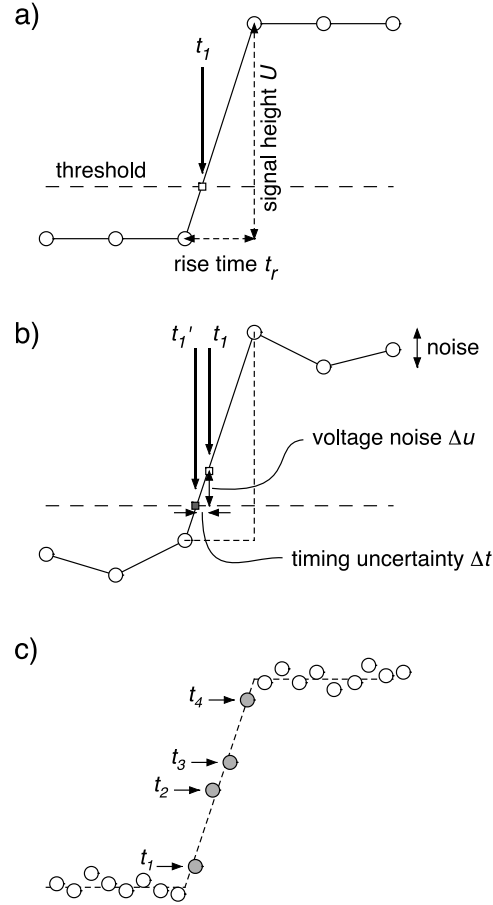


Fig. 2: Time estimations for a leading edge in the ideal case (a), in the presence of noise (b) and for several sampling points lying on the edge (c).

The time resolution can be improved by sampling the signal at a higher frequency. Fig. 2c shows the same signal sampled with four times higher sampling rate. The sampled points scatter around the signal indicated by the dashed line. Now several points lie on the signal edge, shown as grey circles. If the voltage noise of these points is statistically independent (as it is the case e.g. for ADC quantization noise), each point allows a separate measurement of the edge time, and thus reduces the time uncertainty of the edge by \sqrt{n} where n is the number of points lying on the edge. The value of n is also determined by the product of sampling frequency f_s and the signal rise time t_r . This gives the theoretical time accuracy in dependence of the signal-to-noise ratio (SNR) which can be expressed as $\Delta u/U$, the sampling frequency f_s and the signal rise time t_r . Adopting this to (1) and solving for Δt gives

$$\Delta t = \frac{\Delta u}{U} \cdot t_r \cdot \frac{1}{\sqrt{n}} = \frac{\Delta u}{U} \cdot \frac{t_r}{\sqrt{f_s \cdot f_{3dB}}} = \frac{\Delta u}{U} \cdot \frac{\sqrt{t_r}}{\sqrt{f_s}}. \quad (2)$$

From (2) it becomes clear that not only a high sampling frequency is important for a precise time measurement, but also the SNR and the signal bandwidth. It should be noted that (2) is only a simplified formula, since the actual resolution depends on the exact waveform shape and the noise spectrum. It is however a good estimator which has been verified in several applications.

For very fast detector signals, such as pulses from micro-channel plates (MCP) which can have rise times below 70 ps, the rise time gets limited by the bandwidth of the signal chain. The limiting factor can be a pre-amplifier, a long cable or the SCA chip itself, which is further detailed in [4]. The -3dB bandwidth f_{3dB} determines the signal rise time seen by the SCA as

$$t_r \cong \frac{1}{3f_{3dB}}. \quad (3)$$

Putting this into (2) results in the time accuracy in dependence of the bandwidth f_{3dB} as

$$\Delta t = \frac{\Delta u}{U} \cdot \frac{\sqrt{t_r}}{\sqrt{f_s}} = \frac{\Delta u}{U} \cdot \frac{1}{\sqrt{3f_s f_{3dB}}}. \quad (4)$$

Case	U [mV]	Δu [mV]	t_r [ns]	f_{3dB} [MHz]	f_s [GSPS]	Δt [ps]
a)	10	1	1	333	5	45
b)	450	1	1	333	5	1
c)	100	1	0.35	950	5	2.6
d)	500	0.35	1.6	-	5	0.5
e)	63	0.35	0.2	-	5	1.1

Table 1: Theoretical limit of the achievable time resolution Δt for certain signal and sampling parameters.

Table 1 lists various scenarios, which are relevant for this paper. Cases a) – e) assume a typical environmental or preamplifier noise Δu of 1 mV, or a SCA internal noise in case of the DRS4 of 0.35 mV and a sampling speed of 5 GSPS. Assuming a rise time of 1 ns, which is typical for many photomultipliers, it becomes clear that small signals in the 10 mV range will never give a time accuracy better than a few ten ps. Only a significantly higher signal – for example by means of a low-noise, fast preamplifier – can bring the resolution into the picosecond range. If one uses even faster pulses, the bandwidth gets limited by the SCA itself at some point. In the case of the DRS4 chip this bandwidth is 950 MHz, which limits the time resolution for a SNR of 100:1 to 2.6 ps (case c). Case d) and e) are relevant for the TC in chapter IV.B., which is performed with a 100 MHz sine wave with an amplitude of about 1V.

IV. MATERIALS AND METHODS

The TC methods were evaluated with the DRS4 Evaluation Board version 3 (board A) with 12 bits, 5 GS/s and 4 channels

provided by PSI and the DRS4-chip based V1742 (board B) with 12 bits, 5 GS/s and 32 channels, provided by CAEN, Italy.

We further compared the performance results of board A & B with a LeCroy Wave Runner 6050A Oscilloscope (board C) with 8 bits, 5 GS/s and 4 channels and with the V1751 (board D) with 2 GS/s, 10 bits and 4 channels provided by CAEN. In this Paper the presented measurements of board A, B and C were taken at a sampling speed of 5 GSPS, while board D used a sampling speed of 2 GSPS.

A. Voltage Calibration

Since voltage errors and time errors on a SCA chip are correlated, it is important to correct for any voltage error before a TC can be done.

The voltages of the stored waveform show slightly different offsets and gains for each sampling cell. In the DRS4 chip, this comes mainly from the fact that each sampling capacitor is read out by a separate buffer, which has a typical offset of 10-20 mV. These offsets can be measured by connecting the input to a DC voltage, e.g. 0 V, and then subtracting these offsets in each measurement as a voltage correction.

It is important to do the offset calibration at the same voltage level as used later for time measurements. In board B an external bias offset gets applied to shift the input range of the DRS4 chip after the voltage calibration. As shown in Fig. 11, this caused a small error in the voltage calibration and then degrades time measurements.

The gain calibration for each cell is done by applying a DC voltage of 800 mV to the input and measuring the response of the cell. This additional correction is performed for board A but not for board B.

B. Time Calibration (TC)

The sampling intervals of the DRS4 chip are not equidistant, but constant over time. This means the DRS4 has to be calibrated before a precise time measurement can be made. In this paper the time calibration from board A will be named TC A and the TC from board B will be called TC B. Consistently, the new TC will be referred to as TC N.

In the following we will use Δt_i as the effective sampling interval between cell# i and cell# $i+1$. We define Δt_i as the time difference between the opening of the analogue switches $S_{0,i}$ and time point $S_{0,i+1}$ as illustrated in Fig. 1. In order to calibrate a SCA correctly, every channel has to be calibrated individually. From this follows that the integrated or “global” time difference between cell# k and cell# n is given by:

$$\Delta t_{k,n} = \sum_{i=k}^{(n-1)} t_i. \quad (5)$$

For TC N a 100 MHz sine wave with a 1V peak-to-peak value was used in the DRS4 case, when sampling at 5 GSPS. The frequency of the sine wave should be adjusted accordingly to the sampling speed range of the SCA. For the DRS4 case, we recommend a 30 - 40 MHz frequency in order to achieve best timing results independent of the sampling

speed. The TC N consists of two parts. The first part estimates the effective sampling intervals Δt_i by measuring voltage differences between two neighboring cells and is called “local” TC. The second part refines the sampling intervals by measuring time differences between cells that are far apart and is therefore called “global” TC.

1) Local TC

Our approach is that Δt_i is proportional to the measured voltage difference between neighboring cells when applying a linear increasing or decreasing signal, such as a saw-tooth waveform for example. The intercept theorem results in (6) and is illustrated in Fig. 3:

$$\frac{\Delta t_i}{\Delta U_i} = \frac{\Sigma \Delta t_i}{\Sigma \Delta U_i}, \quad (6)$$

where ΔU_i is the voltage difference between cells i and $i+1$. For a SCA with n cells we know

$$\sum_{i=1}^n \Delta t_i = \frac{n}{f_{SCA}}, \quad (7)$$

where f_{SCA} is the nominal sampling frequency of the SCA. Combining (6) and (7) we can calculate all n time intervals Δt_i as:

$$\Delta t_i = \frac{\Delta U_i \cdot \frac{n}{f_{SCA}}}{\Sigma \Delta U_i}. \quad (8)$$

The exact sampling speed f_{SCA} that might deviate from the nominal one is not required since it will be determined in the global TC afterwards.

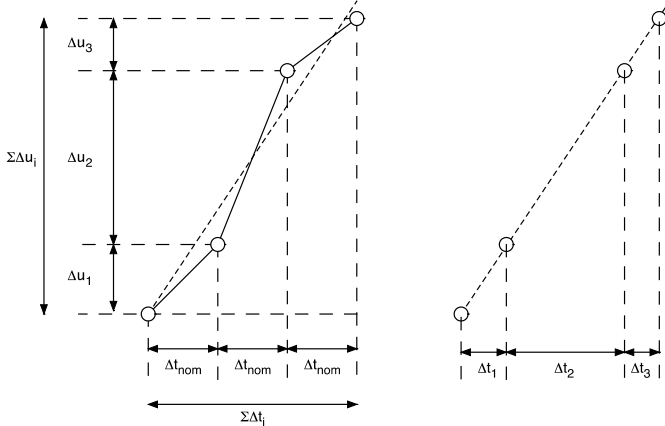


Fig. 3: The correlation between voltage differences ΔU_i and time differences Δt_i of a rising edge can be used for the local TC of a SCA chip.

Using rising and falling edges of the TC signal will result in two calibrations. Averaging over these two calibrations will cancel any residual voltage offset:

$$\Delta t_i = (\Delta t_{i,falling} + \Delta t_{i,rising}) \cdot \frac{1}{2}, \quad (9)$$

Where $\Delta t_{i,falling}$ and $\Delta t_{i,rising}$ stand for the time differences calculated by the falling and rising edges, respectively. Tests

have indicated that using the rising and falling edges of a sine wave like the one in Fig. 4 are good enough to obtain an acceptable local TC. In a digitized waveform only the Δt_i for cells on the slopes of the sine wave can be determined. The procedure therefore has to be repeated for several sine waves with a random phase relative to the SCA clock. 1000 digitized sine waves give a decent result for the local TC.

2) Global TC

The global TC measures one or more periods of the same sine wave used in the local TC. Since the sampling points are unlikely at zero volts, the period is determined by linearly interpolating sampling points below and above zero volts and measuring the time between the intersections of the interpolated lines with the zero line as shown in Fig. 4. In this example the zero crossing is between cells #25 and #26 and between cells #45 and #46, leading to two corrections

$$t_{cor} = \frac{U_k}{\Delta U_{k-1}} \Delta t_{k-1} - \frac{U_n}{\Delta U_n} \Delta t_n, \quad (10)$$

which constrain the time between the cell# $k = 26$ and cell# $n = 45$ using the known period time of the digitized sine wave T_{sin} as in

$$m \cdot T_{sin} \stackrel{\text{def}}{=} t_{k,n} + t_{cor}, \quad (11)$$

where m stands for the factor describing the multiples of the measured periods. U_i is the voltage measured at cell# i .

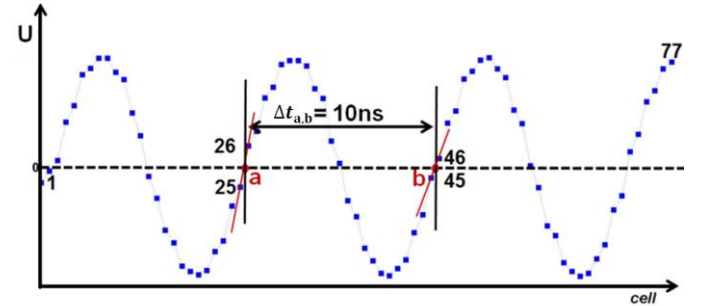


Fig. 4: First 77 cells of the 1024 cell array of a DRS4 sampling a 100 MHz sine wave at a sampling speed of 2.5 GSPS. This signal is used for the local TC and the global TC.

In Fig. 4 the global time difference $\Delta t_{a,b}$ has to be $1 \cdot 10$ ns. The two points a and b are artificial points and stand for the zero crossings of two rising edges of the digitized sine wave.

Finally the global TC is computed iteratively by correcting the local TC each time we measure a multiple of the period time $m \cdot T_{sin}$.

$$\begin{aligned} \Delta t_{k,new} &= \Delta t_k \cdot u_{cor} \\ \Delta t_{k+1,new} &= \Delta t_{k+1} \cdot u_{cor} \\ &\vdots \\ \Delta t_{n-1,new} &= \Delta t_{n-1} \cdot u_{cor} \end{aligned} \quad \text{with} \quad u_{cor} = \frac{m \cdot T_{sin}}{t_{k,n} + t_{cor}}, \quad (12)$$

where $\Delta t_{k,new} \dots \Delta t_{n-1,new}$ stand for the corrected effective sampling interval. $\Delta t_k \dots \Delta t_{n-1}$ stand for the old data set of effective sampling intervals that are going to be corrected. The first iteration will start with the data set provided by the local TC (8). In the following iterations the $\Delta t_{i,new}$ provided by (12) will be used as Δt_i in order to apply (12) again every time a new $t_{k,n}$ is measured. Iterating over typically 1000 digitized sine waves is usually enough to obtain a precise global TC. For practical reasons, the measured sine waves in the local TC can be “recycled” for the global TC if their time values are replaced with the new ones. In Table 1 case e) one can see that the expected time resolution is about 1.1 ps for a single interpolation, when using the 100 MHz sine wave. In this case the voltage difference between sampling points of a rising edge is in average about 63 mV with an average sampling interval of 0.2 ns.

C. Board Time Resolution Test

To examine the time resolution of the four boards and the quality of TC N, 4 different performance tests were applied. The time resolutions for all performance tests are given in root-mean-square (RMS).

1) The Period Time Test (PT-test)

The 100 MHz sine wave used for the TC N was applied for the PT-test, too. Fig. 5 shows the measured period time between two zero crossings of the rising edges which should be equal to 10 ns. The period time is plotted over the cell number that is left of the first zero crossing. Thus, $\Delta t_{a,b}$ from Fig. 4 would be represented by cell# 25 in Fig. 5. The top plot shows the time for an uncalibrated DRS4 chip, the middle after the local TC and the bottom after the global TC. While the local TC effectively corrects variations between neighboring cells, a residual inaccuracy with more global structures is left over, which can be seen in the middle plot. The global TC then corrects these global structures, which leads to a flat distribution shown in the bottom plot. This method is therefore very powerful to determine the accuracy of the TC.

In Table 2 - Table 5 we compare the distribution of the period time (i.e. the projection of the distribution in Fig. 5 bottom onto the Y-axis) for different hardware. The 100 MHz sine wave amplitude was 1V peak-to-peak. For each measurement 10000 events were digitized and averaged.

2) The Split Pulse Test (SP-test)

We evaluated the actual time precision for the tested 4 boards as shown in Fig. 6 with the SP-Test. A short pulse is generated by a function generator. The signal is split and the time difference between the arrivals of the two signals is measured. We changed the arrival time of one of the signals by applying a variable cable delay (Fig. 6 and Fig. 7).

In most cases we used a simple Digital Leading Edge (DLE)-discriminator to evaluate the time resolution.

3) The Coincident Resolving Time Test (CRT-test)

Fig. 8 shows the setup of a PET time resolution measurement (CRT) when using the DRS4 chip with and without applying

TC N instead of TC B. We used two 5mm · 5mm · 5mm LSO:Ca crystals as scintillators glued to two fast PMT's (Hamamatsu R10560).

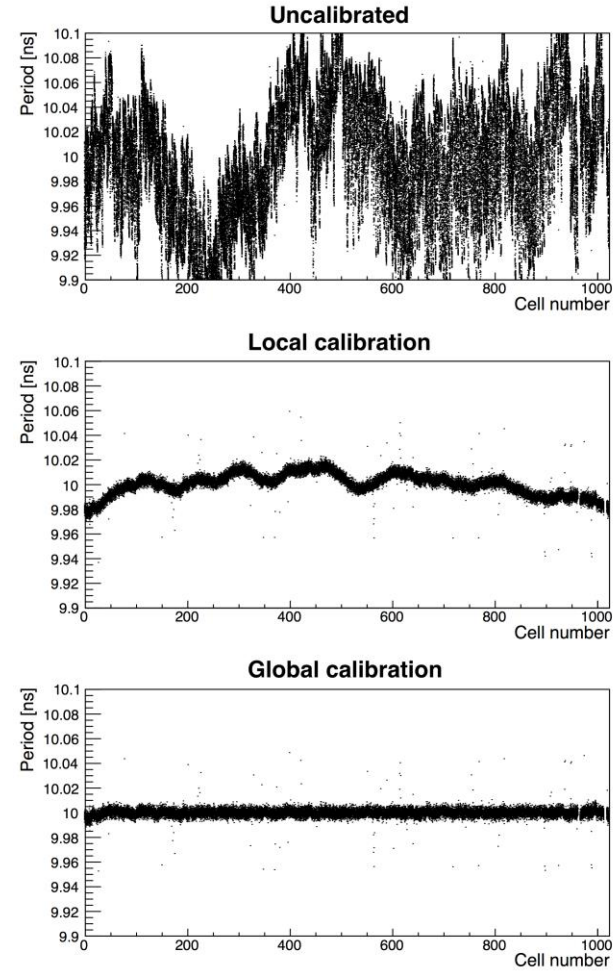


Fig. 5: Effect of the local TC and the global TC when used to determine the period of a 100 MHz sine wave. (PT-test)

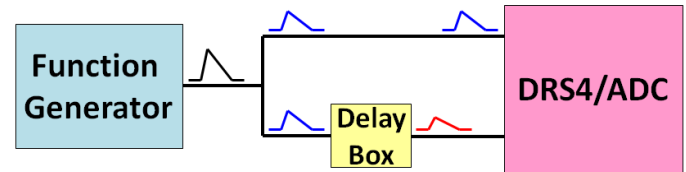


Fig. 6: Layout of the split signal time measurement.

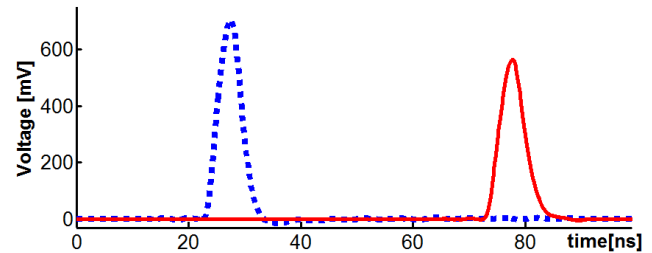


Fig. 7: Split pulse digitized at 5 GSPS for the SP-test with board C and a full range of ~1.1V. The dotted signal height peaks around 720 mV and the delayed solid line peaks at around 610 mV due to attenuation. The time difference between the signals is approximately 50 ns.

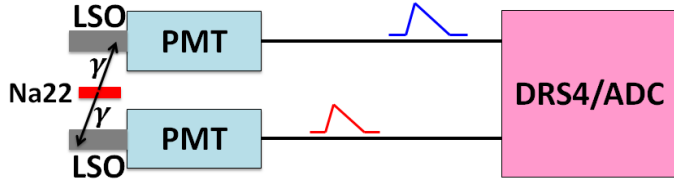


Fig. 8: Layout for the PET time measurement.

4) The Temperature Time Dependence Test (TTD-test)

For the TTD-test board A was used with TC N. The global time difference $\Delta t_{15,468}$ between cell# 15 and cell# 468 was measured at 8 different temperature levels from 5 °C to 40 °C.

V. RESULTS

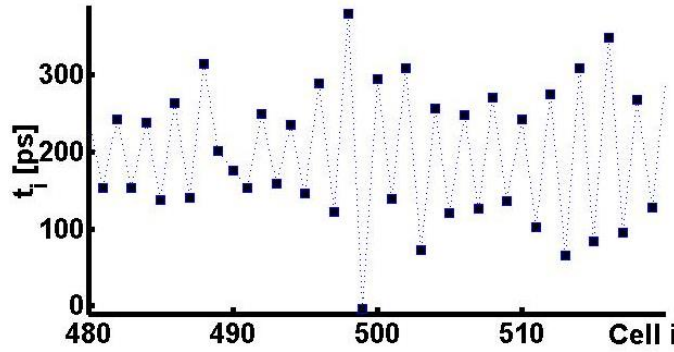


Fig. 9: Effective sampling intervals Δt_i of 40 arbitrary cells after applying TC N for channel# 4 of board A.

The sampling intervals of adjacent cells differ by about 100 ps for the DRS4 from the nominal width of 200 ps at 5 GSPS, which can be seen on the slopes of the waveform in Fig. 4. In Fig. 9 one can see that this DRS4 chip has alternating sampling intervals with extremes at $\Delta t_{497} = 370$ ps and $\Delta t_{498} = -3$ ps. A negative bin width means that the signal reaches cell# 499 before it gets sampled in cell# 498 which can be explained by the layout of the chip. By using the TC N we verified that board B is running at the nominal 5 GSPS and board A has a slight variation. More details are given in section VI.

8 bit- Range [mV]	Baseline-Noise		Mean Value		RMS	
	ch1 [mV]	ch2 [mV]	ch1 [ps]	ch2 [ps]	ch1 [ps]	ch2 [ps]
1126.7	5.21	4.42	9999.99	9999.95	20.8	16.7(14)
225.4	1.03	0.87	10000.08	10000.01	5.2	4.6(2.8)
112.5	0.57	0.48	10000.08	10000.02	3.9	3.6(1.5)

Table 2: PT-test results for board C with 3 different gains. The theoretical best time resolution for channel# 2 according to formula (1) is shown in brackets.

Table 2 shows the results for the oscilloscope (board C). The resolution can be improved by increasing the gain, but

with the drawback of a clipped signal. The full signal was only visible in the first case on the oscilloscope screen (100 MHz sine wave with 1V amplitude) and results for channel# 2 in a time resolution of 16.7 ps. By increasing the gain the information of the full waveform got lost but increased the time resolution. The best gain uses the 8 bits for a full range of 112.5 mV and achieved a time resolution of 3.6 ps. Increasing the gain further would cause some loss of information at the zero crossings and degrade the resolution again.

12 bit- Range [mV]	Baseline-Noise		Mean Value		RMS	
	ch1 [mV]	ch2 [mV]	ch1 [ps]	ch2 [ps]	ch1 [ps]	ch2 [ps]
1000.0	0.43	0.45	9999.99	9999.97	3.11	3.23(1.4)

Table 3: PT-test results for board A with TC N for channel# 1 and for channel# 2. The theoretical best time resolution for channel# 2 according to equation (1) is shown in brackets.

Table 3 shows that board A gives a better time resolution for the PT-test than board C (Table 2). Both boards show the expected period time of about 10 ns.

TC N for ch1		TC N for ch2		TC A	
Mean [ps]	RMS [ps]	Mean [ps]	RMS [ps]	Mean [ps]	RMS [ps]
9999.99	3.11	9999.97	13.20	100004.54	48.05

Table 4: PT-test results for board A with 3 different TCs always applied to the same dataset measured with channel# 1.

In Table 4 we also see that TC N is about 15 times better than TC A and also provides the correct period time of 10 ns, even when TC N for channel# 1 is applied to channel# 2.

TC N for	ch1 RMS [ps]	ch2 RMS [ps]	ch3 RMS [ps]	ch4 RMS [ps]
ch1	3.11	13.20	14.35	14.84

Table 5: PT-test results for the four channels of board A, where TC N for channel# 1 is applied to channel# 1 to channel# 4.

Table 4 and Table 5 demonstrate that that every channel has to be calibrated individually to obtain a time resolution below 10 ps.

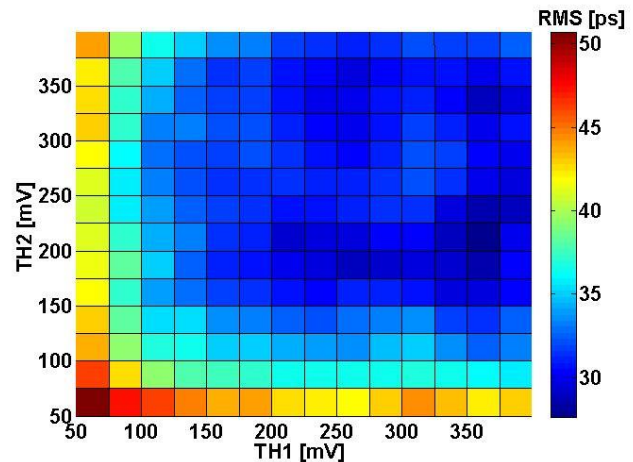


Fig. 10: SP-test obtained with board C with 50 ns delay.

The results for the SP-test of a 50 ns delay are shown in Fig. 10 and Fig. 11. The effect of using a wrong offset calibration level with the DRS4 is illustrated in Fig. 11. We shifted intentionally the baseline by applying a 400 mV DC offset. Fig. 10 shows the time resolution result of the SP-test for board C in dependence on the first threshold TH1 (first signal) and the second threshold TH2 (second signal) of the used digital leading edge (DLE) discriminator. The optimum time resolution is 28 ps (RMS) with the signal shown in Fig. 7 was digitized with 8 bit resolution and a full range of ~ 1.1 V.

The optimal time resolution of board B as shown in Fig. 11 is 4.6 ps (RMS) when using TC N. The same signal as shown in Fig. 7 is now digitized with 12 bit resolution. As expected the best TH2 level is lower than the optimal TH1 level, since the split signal is 15 % smaller in the second. When running the DRS4 of board B at a different DC offset level the resolution would be improved to < 3 ps as shown in Fig. 12.

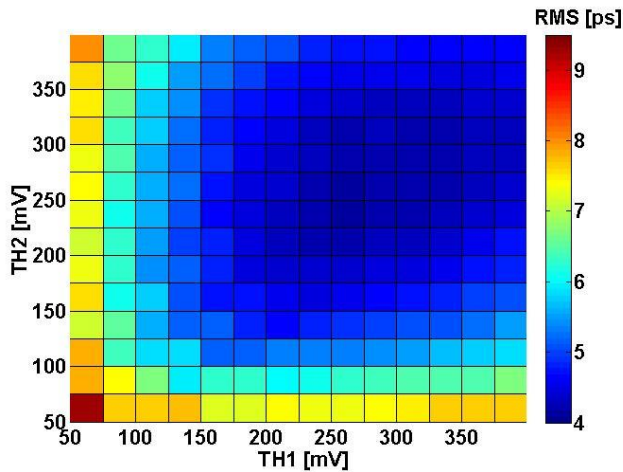


Fig. 11: SP-test with the same delay as in Fig. 10 for board B.

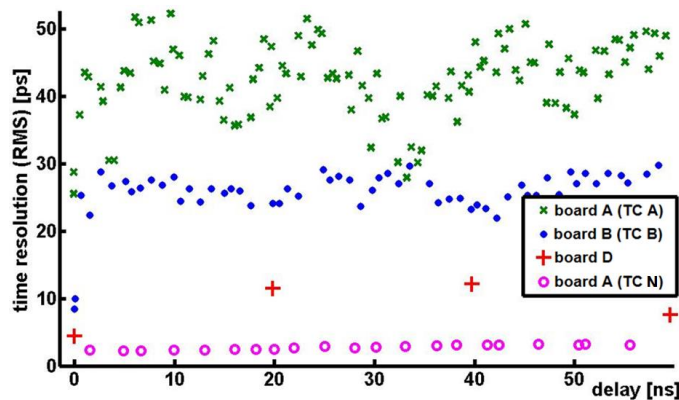


Fig. 12: SP-test measurements obtained for 3 different boards.

Fig. 12 illustrates results of a SP-test, where the time resolution in dependency of the delay is shown. Board D (large crosses) was running at 2 GSPS with a resolution of 10 bits. The two other boards were running at 5 GSPS using the DRS4 chip. The x symbols mark the results of Board A using TC A and indicate a time resolution variation from 25 ps to 55 ps. The same board achieves a time resolution of about 3 ps for all delays when TC N was applied (circles). The dots stand for the measurement points of board B using TC B. The DLE-discriminator was used in all four cases.

Fig. 13 shows a zoom-in of the board A (TC N) curve from Fig. 12. For the same dataset two additional analysis methods are also shown. The circles and the dots were calculated with a DLE-discriminator. This basically means that the split signals (Fig. 7) were baseline corrected and fitted using 2 points and 6 points, respectively. The time information was then obtained at a TH of 300 mV for both channels. For the 50-points measurement (crosses) a cross-correlation between the two signals was used. One can see that the time resolution progresses when using more points. The time resolution curve shows approximately a linear rising behavior for all three cases.

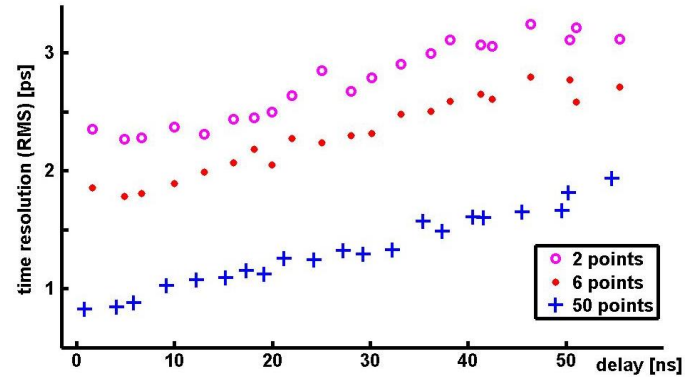


Fig. 13: SP-test measurements with board A after applying the TC N method. The same dataset was analyzed three times using different techniques.

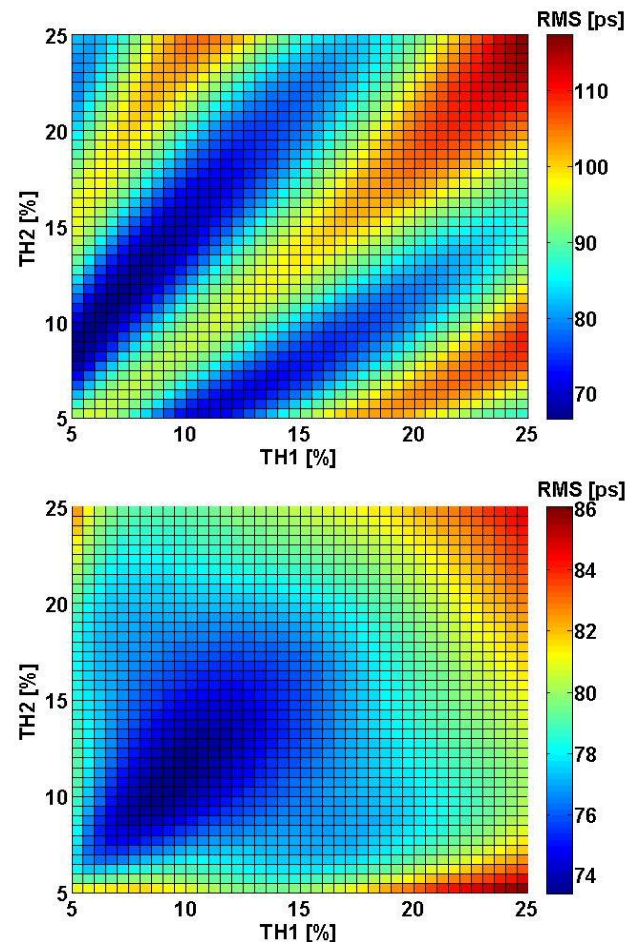


Fig. 14: Results for the CRT-test measured with board B. Two measurements with changing from TC B (top) to TC N (bottom) were performed.

Fig. 14 shows two time resolution results of the CRT-test as a function of the thresholds TH1 (PMT# 1) and TH2 (PMT# 2) of the used DLE discriminator. TH1 and TH2 are given in percentage of the average photo peak height of the particular channel. 65 ps CRT (RMS) with TC B for best THs was measured and 74 ps CRT (RMS) with the TC N. See Discussion for more details.

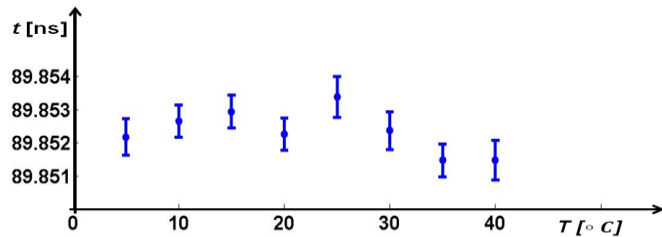


Fig. 15: TTD-test of board A. For each of the 8 measurements 1000 digitized waveforms were analyzed. In average about 85 events could be used each time to compute the global time difference $\Delta t_{15,468}$.

In Fig. 15 the temperature dependency of the time resolution of the DRS4 chip is plotted. One can see that $\Delta t_{15,468}$ is varying less than 2 ps.

VI. DISCUSSION

By using TC N for the DRS4 chip we discovered that the true value of the sampling intervals Δt_i alternate between 130 ps and 270 ps with a RMS of ~ 23 ps at 5 GSPS (Fig. 9). The reason for these alternations lies in the layout of the DRS4 chip, where odd and even cells see a different environment on the chip die. At lower sampling speeds one will find a similar alternating behavior of the DRS4 chip. Since the signal edges between the inverters have longer rise times at lower sampling speed, internal noise plays a bigger effect and the timing performance degrades about inversely with the sampling frequency $\Delta t \sim 1/f_s$.

The PT-Test in Table 3 shows that TC N for board A yields in the expected period time of 10 ns and a time resolution of 3.1 ps. With the best gain, board C only reaches 3.6 ps (Table 2). Since the time resolution is proportional to the rise time of the signal at a given signal-to-noise, a higher gain setting for board C results in a better time resolution, although the peaks of the test-signal will then be clipped.

The channel-by-channel TC (illustrated in Table 4 and Table 5) can be understood by looking at Fig. 1. Every analog switch connected to the sampling capacitors has a separate buffer. The transition times of these buffers are different due to the above-mentioned variations in chip process parameters.

Board A had issues before with measuring long time differences [15]. This problem is now understood and has two reasons. First, the true sampling speed differed from the nominal one by about 0.01 %. The measurement of the true sampling speed with TC N and the usage of a more precise oscillator with less jitter on version 5 of board A solved this problem. Second, a 2.5 MHz digital signal on board A on a PCB trace close to the DRS4 chip induced some instability of the PLL inside the DRS4 which lead to two distinguished alternating sampling speeds. A redesign of the PCB with a

better shielding of this signal fixed that problem.

Looking at the 50 ns delay result from Fig. 13 compared to Fig. 11 shows a time resolution drop from 2.9 ps to 4.6 ps for the same measurement when using a different offset level. We used a DLE-Discriminator where the stability of the baseline is mandatory. This underscores again that the nominal voltage non-linearity of the DRS4 chip of 0.5 mV (see data sheet [16], Plot 2) has a considerable effect on the time resolution. A cell-by-cell calibration of the non-linearity could therefore improve the time resolution even further.

Under similar conditions board C achieved 28 ps (Fig. 7). This was predictable since it only uses 8 bits for a full range of ~ 1.1 V (Table 2 & Table 3). The best time resolution for board C performing the SP-test was around 8 ps, when the gain was increased by a factor of 10 to a full range of 0.1125 V, but with the penalty of above-mentioned clipping.

Fig. 12 shows the SP-test for different boards and TCs. In comparison to TC B the TC A on board A is about two times worse. This is mainly caused by the TC-signal that was used for the TC A, which has a jitter greater than 100 ps. Also, the time resolution should remain constant when increasing the delay, which is not the case for TC A or TC B. Instead, the DRS4 digitizers show a strong correlation between the delay and its corresponding time resolution behavior when using TC A or TC B.

The large DRS4 time resolution improvement when comparing TC N with the other TCs can be explained with the following: When looking at the time axes of an uncalibrated channel running at 5 GSPS, the maximal error is around 800 ps. When comparing TC N with TC A or TC B, the maximum error is still around 150 ps. This is because the other TCs provide almost equidistant sampling intervals of 200 ps with a RMS of 3 ps and not the alternating behavior mentioned at the beginning of section VI. However, one can also see in Fig. 12 that after using TC N, the curve for board A lies under the curve of board D as expected, because the DRS4 was running at 5 GSPS using 12 bits and board D at 2 GSPS using 10 bits.

In Fig. 13 one can see that the time resolution is improved by using more sampling points of the signal, as expected. The increase of the time resolution with the cable delay comes from the fact that the sampling speed varies around its nominal value due to the residual phase jitter of the PLL in the DRS4 chip. This can be seen in Fig. 16 which shows the deviation of the sampling time from the exact time due to the PLL time jitter. If two signals are sampled at times t_1 and t_2 on separate channels driven by the same inverter chain, their deviation from the perfect time is Δt_1 and Δt_2 , respectively. The relative time error between the two signals is Δt , which is proportional to the time distance $t_2 - t_1$ as long as the time difference is smaller than the clock period. Since the inverter chain in case of the DRS4 is 1024 cells long, the time resolution in Fig. 13 increases from 0.8 ps at 0 ns delay (which is close to the theoretical optimum) to 4.8 ps at 200 ns delay (extrapolated), reflecting the PLL jitter of about 4 ps.

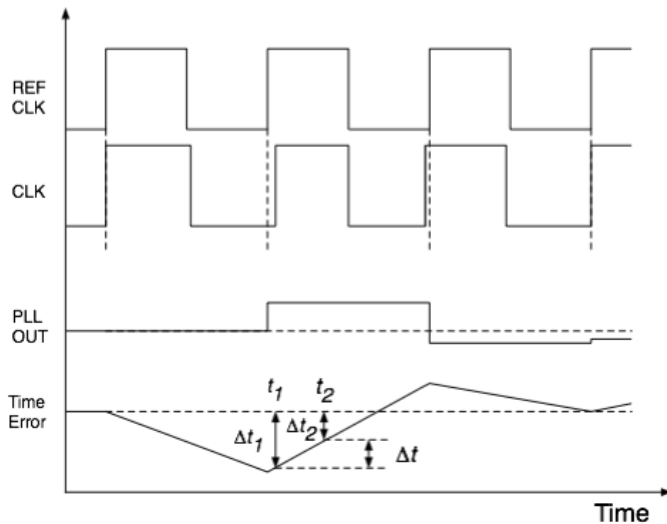


Fig. 16: PLL phase jitter in a SCA chip. REFCLK is the external (exact) reference clock, CLK the frequency of the inverter chain, PLLOUT is the control voltage from the PLL and Time Error the deviation of the sampling time from the exact time.

In Fig. 14 the importance of applying TC N is shown with an example of a real PET measurement (Fig. 8). Looking at measurements of board B using TC B one will get a wrong result. This is illustrated in the top figure of Fig. 14, which shows 3 minima instead of just one expected and is 7 ps better CRT (RMS) than possible. We know that the time resolution result of the board B (TC B) is wrong because we double checked the experiment with an oscilloscope with 20 GSPS and an adjusted gain for a comparable 12 bit resolution. Although we digitized 4 times faster, we only archived a CRT (RMS) of 72 ps for best threshold (TH) settings. The reason for the wrong result is the following:

We know that the effective sampling interval Δt_i of TC B provides almost equidistant 200 ps sampling intervals. As mentioned above the true Δt_i alternates between 130 ps and 270 ps. When changing the TH settings as shown Fig. 14 one will also measure different time differences between the two PET signals (walk effect). The three minima also represent regions of similar time differences. When this time difference is calculated by interpolating between two neighboring cells that are mainly 270 ps apart but wrongly considered to be 200 ps, the calculated RMS will be smaller than in reality and will therefore result in a wrongly considered as better time resolution result.

The temperature stability test of board A in Fig. 15 shows that the time jitter is less than 1-2 ps in a temperature range from 5°C to 40°C.

Ultimately, we plan to improve the board A and B

performance by working on an advanced voltage calibration.

VII. CONCLUSION

The novel TC N gives excellent results for SCA-based time measurements and is applicable also for other chips than the DRS4.

In the DRS4 case a time resolution improvement by a factor of 8 to 15 has been achieved. The performance is now much better compared to an oscilloscope, while the costs of a SCA-based system are one order of magnitude lower. Up to 30 ns delay (Fig. 13) the time resolution of the DRS4 is below 1.4 ps, giving a single time resolution better than $1.4 \text{ ps}/\sqrt{2} = 1 \text{ ps}$.

Thus, the DRS4 provides an excellent measurement platform for applications in particle physics or in PET medical imaging.

ACKNOWLEDGMENT

The authors would like to thank the colleagues from Siemens Medical Imaging, especially Matthias Schmand, Nan Zhang, Robert Mintzer, Sanghee Cho, Peter Cohen and Larry Byars for supporting the work with the DRS4.

We are also grateful to Ueli Hartmann, Christoph Parl, Chih-Chieh Liu, Frederic Mantlik, Armin Kolb, Mathew Divine and Jeanine Adam for helpful conversations and/or support.

We would like to thank the University Hospital Tübingen for making it possible to file in an international patent application (No. PCT/EP2013/070892) containing several TCs including the demonstrated new TC method.

REFERENCES

- [1] S.A. Kleinfelder, IEEE Trans. Nucl. Sci. NS-35 (1988) 151
- [2] G.M. Haller, B.A. Wooley, IEEE Trans. Nucl. Sci. NS-41 (1994) 1203
- [3] E. Delagnes et al., Nucl. Instr. Meth. A 567 (2006) 21
- [4] G.S. Varner et al., Nucl. Instr. Meth. A 583 (2007) 447
- [5] S. Ritt et al., Nucl. Instr. Meth. A 623 (2010) 486
- [6] E. Oberla et al., Nucl. Instrum. Meth. A 735 (2014) 452
- [7] J. Adam et al., Eur. Phys. J. C73 (2013) 2365
- [8] J. Sitarek et al., Nucl. Instr. Meth. A723 (2013) 109
- [9] D. Breton et al., IEEE Nucl. Sci. Symp. Conf. Rec. (2010) 856
- [10] M. Ageron et al., Nucl. Instr. Meth. A 622 (2010) 59
- [11] B. W. Jakoby et al., Phys. Med. Biol., 56 (2011) 2375
- [12] D.R. Schaart et al., Phys. Med. Biol., 55 (2010) 179
- [13] D. Breton et al., Nucl. Instr. Meth. A 629 (2011) 123
- [14] A.M. Makankin et al., Nucl. Instr. Meth. A 735 (2014) 649
- [15] A. Ronzhin et al., Nucl. Instr. Meth. A 668 (2012) 94
- [16] DRS4 data sheet, http://www.psi.ch/drs/DocumentationEN/DRS4_rev09.pdf